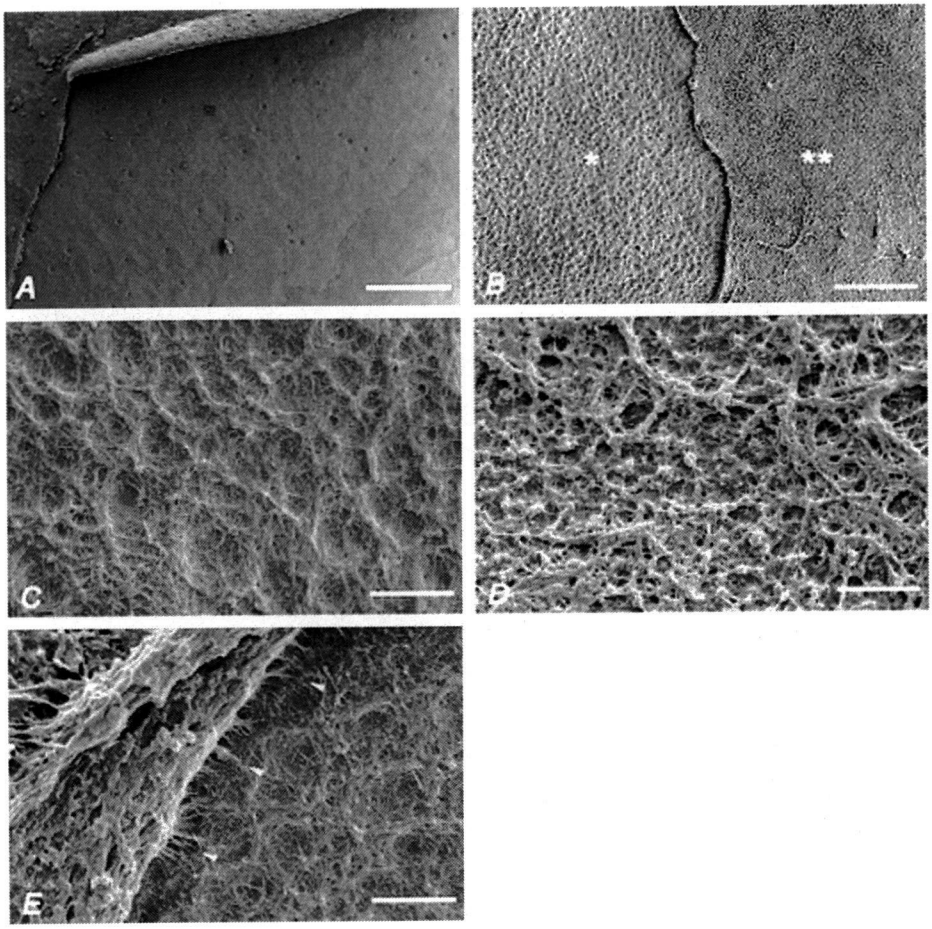

Figure 7. *A*: Scanning electron micrograph of a stromal bed after mechanical separation at low magnification (×50) (*bar* = 200 μm). *B*: Magnified view (×1000) of panel *A* (*bar* = 20 μm) shows partially exposed Bowman layer (*single asterisk*) and preserved basement membrane on the surface of the stromal bed in some areas (*double asterisk*). *C*: High magnification (×10 000) of the exposed Bowman layer (*bar* = 2 μm). *D*: High magnification (×10 000) of the remaining basement membrane on the stromal bed (*bar* = 2 μm). *E*: Magnified view (×10 000) of the interface between the basement membrane and Bowman layer shows numerous fibers adhering to both regions (*arrowheads*) (*bar* = 2 μm).

interface between the regions of the lamina densa and Bowman layer, numerous fibrils, likely the lamina fibroreticularis, adhered to both regions (Figure 7, *E*). No cleavage planes within Bowman layer or the corneal stroma were observed in the 4 eyes.

Transmission electron microscopy of the stromal beds showed 2 distinct cleavage planes, 1 at the level of the lamina fibroreticularis and the other at the level of the lamina lucida. In the former, portions of the lamina fibroreticularis that were approximately 100 to 200 nm thick were present above Bowman layer, indicating that mechanical separation occurred within the lamina fibroreticularis (Figure 8, *A*). In the latter, bundles of anchoring fibrils and the lamina densa were retained on Bowman layer (Figure 8, *B*), which showed that the epithelial flap was separated along the lamina lucida in these regions. For both cleavage planes, Bowman layer and the stroma had normal morphology with no trauma in either region.

When immunostaining for type IV collagen was performed, positive expression was observed only along the surface of Bowman layer (Figure 9, *A*). In contrast, there was positive staining for type VII collagen in all regions of the stromal surface (Figure 9, *B*). In the stromal beds, expression of integrin α_6 was discontinuous in some areas while other regions had no staining (Figure 9, *C*). Similarly, integrin β_4 showed patchy expression only in some regions of the stromal bed surfaces (Figure 9, *D*). Laminin 5 had discontinuous linear expression along the surface of Bowman layer (Figure 5, *E*). These results indicate that the epithelial flap was cleaved along the lamina lucida where types IV and VII collagens and laminin 5 were expressed and patchy patterns of integrin α_6 and β_4 were observed. These findings suggest that epithelial separation occurred within the upper regions of the lamina lucida. It also appears that the plane of cleavage during the epi-LASIK procedure was within the lamina fibroreticularis, which was negative for type IV collagen, integrin α_6 and β_4, and laminin 5 but positive for type VII collagen.

DISCUSSION

The current study identified 3 major histological characteristics of the epithelial flaps and stromal beds

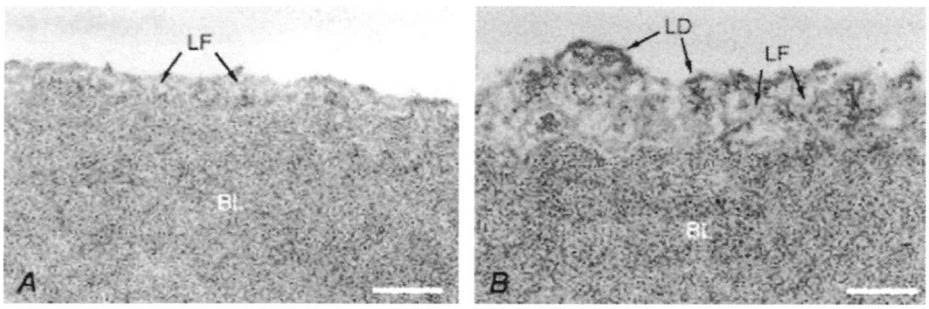

Figure 8. Transmission electron micrographs of stromal beds after mechanical separation. *A*: The lamina fibroreticularis (LF) comprised of anchoring fibrils is preserved at a thickness of 100 to 200 nm on Bowman layer (BL). *B*: The lamina densa (LD) and lamina fibroreticularis (LF) are present on Bowman layer (BL) (*bars* = 200 nm).

created during epi-LASIK using an epikeratome. First, Bowman layer and the underlying corneal stroma remained intact after epithelial separation. Second, the cleavage planes of the epithelial flap and the stromal beds were relatively smooth. Finally, the epithelial flap was mechanically separated at 2 cleavage planes in some regions along the lamina lucida and in the lamina fibroreticularis in other regions.

In the current study, we report what we believe is the first histologic evaluation of the characteristics of the corneal stromal bed after mechanical separation using the Epi-K epikeratome. There was no obvious trauma to Bowman layer or the underlying stroma in the stromal beds after mechanical separation, suggesting that epi-LASIK performed using this epikeratome is safe and avoids complications (eg, microstriae,

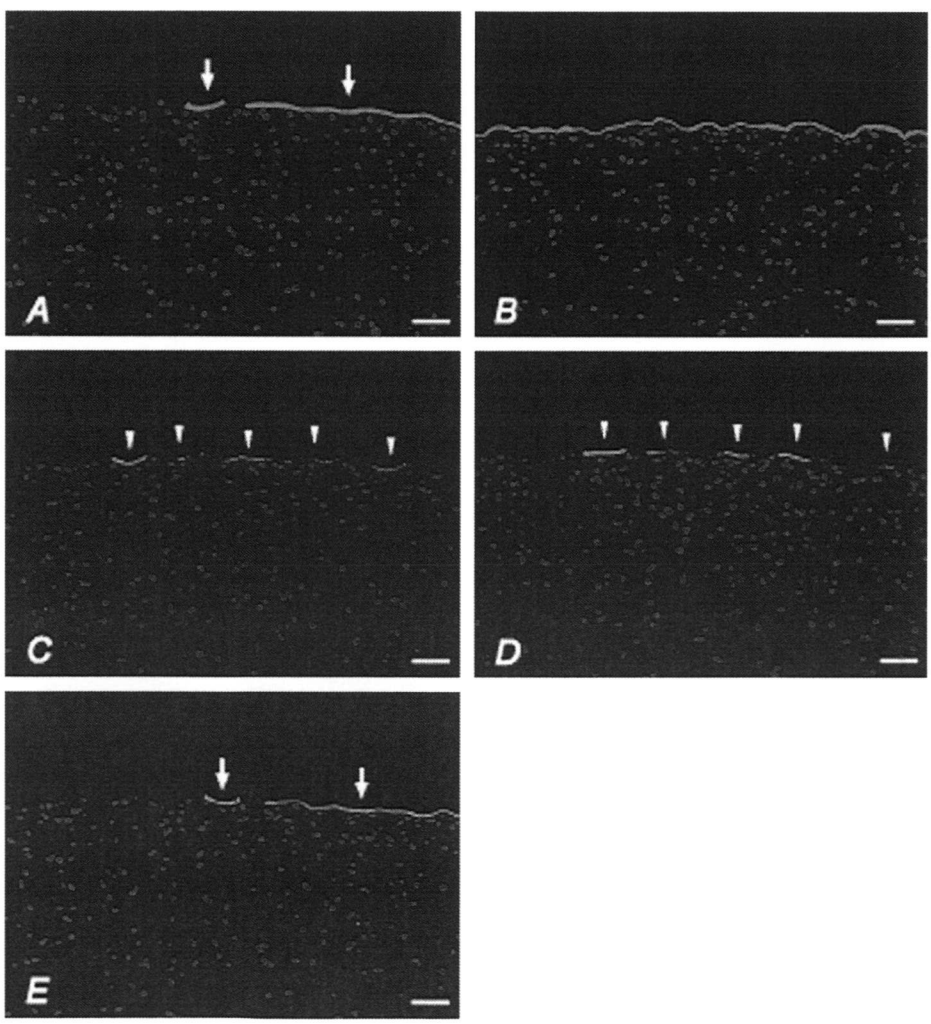

Figure 9. Immunostaining of a stromal bed for types IV and VII collagens, integrin α_6 and β_4, and laminin 5. *A*: Discontinuous positive staining for type IV collagen along the surface of the stromal bed (*arrows*). *B*: Positive staining for type VII collagen in all regions of the stromal bed. *C*: Patchy staining of integrin α_6 along the stromal surface (*arrowheads*). *D*: Patchy staining of integrin β_4 along the stromal surface (*arrowheads*). *E*: Discontinuous positive staining of laminin 5 shows along the surface of the stromal bed (*arrows*) (*bars* = 100 μm).

epithelial ingrowth) that can occur at the stromal interface after LASIK.[3]

We also found that most of the stromal surfaces contained regions with Bowman layer mostly exposed in approximately two thirds of the entire stromal bed area and that portions of the basement membrane, with thickness ranging from 100 to 200 nm, remained on the stromal surface in the other area. These results indicate that mechanical separation with the epikeratome we used provides a relatively smooth underlying bed surface before photoablation. A smooth stromal bed theoretically reduces postoperative corneal haze and irregular astigmatism, which can lead to less predictable visual results.[23] Moreover, compared with LASEK, epi-LASIK may create a similarly smooth stromal surface without use of topical alcohol, which can be toxic to the epithelial flap and stromal bed.

The epikeratome we used separates the epithelial layer from the underlying stroma using 3 speeds. The device is shifted from low speed to medium speed when the epithelial flap rises and from medium speed to top speed when the separator reaches the center of the cornea. Scanning electron microscopy of the stromal beds showed that the portions of the basement membrane were generally seen as island-like formations mainly in the center of the stromal bed, with the surrounding areas having mostly exposed regions of Bowman layer. These island-like formations were almost symmetrical to a straight line parallel to the hinge passing the center of the cornea. In addition, in the peripheral area of the stromal beds, the mostly exposed Bowman layer was seen in the region where the epithelial flap was cleaved initially as well as in the other peripheral regions. This result suggests that change of advance-head speed of the epikeratome we used may not affect separation layers.

Pallikaris et al.[12] assessed epithelial flaps after mechanical separation in epi-LASIK and found that the epithelial layers were separated beneath the basement membrane with intact epithelial basal cells, although they found that the basal epithelial cells rested on the prominent basal lamina with occasional focal disruptions. Katsanevaki et al.[24] also assessed inadvertently dislocated epithelial flaps and found that most epithelial cells were morphologically close to normal with minor cell degeneration. In a study by Kollias et al.,[21] the basal cell layer of the epithelial flap had normal morphology with interruptions of the basement membrane. However, Tanioka et al.[22] report that the basement membrane of the basal cells was partially or totally lost and the membrane of the basal cells was damaged in some regions. Microscopic and immunochemical evaluations in our study showed that epithelial separation occurred at 2 levels: within the lamina fibroreticularis with intact basal cells in some regions and along the lamina lucida with a damaged plasma membrane in other regions. Our results are similar to those reported by Tanioka et al.,[22] but not those of Pallikaris et al.[12] and Kollias et al.[21] Several possible reasons may account for this discrepancy and surgical devices can play a role. We used the same type epikeratome as Tanioka et al.; the type of epikeratome in the other 2 studies was a different model. Other factors, such as surgeon skill, surgical procedure, and corneal conditions, may affect the epithelial flap.

In conclusion, an epi-LASIK procedure using an Epi-K epikeratome mechanically separated the epithelial flap partially along the lamina lucida and within the lamina fibroreticularis in other regions. The device also provided a relatively smooth corneal surface with an intact Bowman layer and stroma after mechanical separation. Further studies are needed to determine which cleavage planes maintain cell viability of the epithelial flap and to enhance epithelial flap survival on the stromal bed postoperatively to reduce pain and haze after epi-LASIK.

REFERENCES

1. El-Maghraby A, Salah T, Waring GO III, Klyce S, Ibrahim O. Randomized bilateral comparison of excimer laser in situ keratomileusis and photorefractive keratectomy for 2.50 to 8.00 diopters of myopia. Ophthalmology 1999; 106:447–457
2. Hersh PS, Brint SF, Maloney RK, Durrie DS, Gordon M, Michelson MA, Thompson VM, Berkeley RB, Schein OD, Steinert RF. Photorefractive keratectomy versus laser in situ keratomileusis for moderate to high myopia; a randomized prospective study. Ophthalmology 1998; 105:1512–1522; discussion by JH Talamo, 1522–1523
3. Gimbel HV, van Westenbrugge JA, Anderson Penno EE, Ferensowicz M, Feinerman GA, Chen R. Simultaneous bilateral laser in situ keratomileusis; safety and efficacy. Ophthalmology 1999; 106:1461–1467; discussion by RK Maloney, 1467–1468
4. Stulting RD, Carr JD, Thompson KP, Waring GO III, Wiley WM, Walker JG. Complications of laser in situ keratomileusis for the correction of myopia. Ophthalmology 1999; 106:13–20
5. Tham VM-B, Maloney RK. Microkeratome complications of laser in situ keratomileusis. Ophthalmology 2000; 107:920–924
6. Autrata R, Rehurek J. Laser-assisted subepithelial keratectomy for myopia: two-year follow-up. J Cataract Refract Surg 2003; 29:661–668
7. Autrata R, Rehurek J. Laser-assisted subepithelial keratectomy and photorefractive keratectomy for the correction of hyperopia: results of a 2-year follow-up. J Cataract Refract Surg 2003; 29:2105–2114
8. Scerrati E. Laser in situ keratomileusis vs. laser epithelial keratomileusis (LASIK vs. LASEK). J Refract Surg 2001; 17: S219–S221
9. Chen CC, Chang J-H, Lee JB, Javier J, Azar DT. Human corneal epithelial cell viability and morphology after dilute alcohol exposure. Invest Ophthalmol Vis Sci 2002; 43:2593–2602. Available at: http://www.iovs.org/cgi/reprint/43/8/2593. Accessed March 11, 2009

10. Kim S-Y, Sah W-J, Lim Y-W, Hahn T-W. Twenty percent alcohol toxicity on rabbit corneal epithelial cells; electron microscopic study. Cornea 2002; 21:388–392
11. Pallikaris IG, Katsanevaki VJ, Kalyvianaki MI, Naoumidi II. Advances in subepithelial excimer refractive surgery techniques: epi-LASIK. Curr Opin Ophthalmol 2003; 14:207–212
12. Pallikaris IG, Naoumidi II, Kalyvianaki MI, Katsanevaki VJ. Epi-LASIK: comparative histological evaluation of mechanical and alcohol-assisted epithelial separation. J Cataract Refract Surg 2003; 29:1496–1501
13. Stepp MA, Spurr-Michaud S, Tisdale A, Elwell J, Gipson IL. α6β4 integrin heterodimer is a component of hemidesmosomes. Proc Natl Acad Sci USA 1990; 87:8970–8974. Available at: http://www.pubmedcentral.nih.gov/picrender.fcgi?artid=55082&blobtype=pdf. Accessed March 11, 2009
14. Tervo K, Tervo T, van Setten G-B, Virtanen I. Integrins in human corneal epithelium. Cornea 1991; 10:461–465
15. Adachi E, Hopkinson I, Hayashi T. Basement-membrane stromal relationships: interactions between collagen fibrils and the lamina densa. Int Rev Cytol 1997; 173:73–156
16. Zagon IS, Sassani JW, Ruth TB, McLaughlin PJ. Epithelial adhesion complexes and organ culture of the human cornea. Brain Res 2001; 900:205–213
17. Beuerman RW, Pedroza L. Ultrastructure of the human cornea. Microsc Res Tech 1996; 33:320–335
18. Pallikaris IG, Kalyvianaki MI, Katsanevaki VJ, Ginis HS. Epi-LASIK: preliminary clinical results of an alternative surface ablation procedure. J Cataract Refract Surg 2005; 31:879–885
19. Dai J, Chu R, Zhou X, Chen C, Qu X, Wang X. One-year outcomes of epi-LASIK for myopia. J Refract Surg 2006; 22:589–595
20. Katsanevaki VJ, Kalyvianaki MI, Kavroulaki DS, Pallikaris IG. One-year clinical results after epi-LASIK for myopia. Ophthalmology 2007; 114:1111–1117
21. Kollias A, Ulbig MW, Spitzlberger GM, Abdallat WH, Froehlich S, Welge-Luessen U, Lackerbauer C-A. Epi-LASIK using the Amadeus II microkeratome; evaluation of cut quality using light and electron microscopy. J Cataract Refract Surg 2007; 33:2118–2121
22. Tanioka H, Hieda O, Kawasaki S, Nakai Y, Kinoshita S. Assessment of epithelial integrity and cell viability in epithelial flaps prepared with the epi-LASIK procedure. J Cataract Refract Surg 2007; 33:1195–1200
23. Weiss RA, Liaw L-HL, Berns M, Amoils SP. Scanning electron microscopy comparison of corneal epithelial removal techniques before photorefractive keratectomy. J Cataract Refract Surg 1999; 25:1093–1096
24. Katsanevaki VJ, Naoumidi II, Kalyvianaki MI, Pallikaris G. Epi-LASIK: histological findings of separated epithelial sheets 24 hours after treatment. J Refract Surg 2006; 22:151–154

First author:
Takeshi Soma, MD

Department of Ophthalmology, Osaka University Medical School, Osaka, Japan

JOURNAL OF TISSUE ENGINEERING AND REGENERATIVE MEDICINE
J Tissue Eng Regen Med 2009; 3: 255–259.
Published online 20 April 2009 in Wiley InterScience (www.interscience.wiley.com) DOI: 10.1002/term.161

RESEARCH ARTICLE

Thoracoscopic cell sheet transplantation with a novel device

Masanori Maeda[1], Masayuki Yamato[1], Masato Kanzaki[2], Hiroshi Iseki[1] and Teruo Okano[1]*
[1]*Institute of Advanced Biomedical Engineering and Science, Tokyo Women's Medical University, 8-1 Kawada-cho, Shinjuku-ku, Tokyo 162-8666, Japan*
[2]*Department of Surgery I, Tokyo Women's Medical University, 8-1 Kawada-cho, Shinjuku-ku, Tokyo 162-8666, Japan*

Abstract

Regenerative medicine with transplantable cell sheets fabricated on temperature-responsive culture surfaces has been successfully achieved in clinical applications, including skin and cornea treatment. Previously, we reported that transplantation of fibroblast cell sheets to wounded lung had big advantages for sealing intraoperative air leaks compared with conventional materials. Here, we report a novel device for minimally invasive transplantation of cell sheets in endoscopic surgery, such as video-assisted thoracoscopic surgery (VATS). The novel device was designed with a computer-aided design (CAD) system, and the three-dimensional (3D) data were transferred to a 3D printer. With this rapid prototyping system, the cell sheet transplantation device was fabricated using a commercially available photopolymer approved for clinical use. Square cell sheets (24 x 24 mm) were successfully transplanted onto wound sites of porcine lung placed in a human body model, with the device inserted through a 12 mm port. Such a device would enable less invasive transplantation of cell sheets onto a wide variety of internal organs. Copyright © 2009 John Wiley & Sons, Ltd.

Received 18 October 2008; Revised 11 January 2009; Accepted 21 January 2009

Keywords cell sheet; transplantation; video-assisted thoracoscopic surgery; minimal invasive surgery; rapid prototyping system; pneumothorax

1. Introduction

Temperature-responsive culture dishes on which a temperature-responsive polymer, poly(*N*-isopropylacrylamide) (PIPAAm), is covalently immobilized, enable non-invasive harvesting of cultured cells and the fabrication of transplantable cell sheets (Yang *et al.*, 2005). The surfaces are relatively hydrophobic to allow cell adhesion, spreading and proliferation at 37 °C. However, upon reducing the temperature below 32 °C, the surface becomes hydrophilic in nature, causing cell detachment. Therefore, cells cultured on the surfaces detach without a need for proteolytic enzymes such as trypsin (Yamada *et al.*, 1990). When confluent cells on the surfaces are subjected to temperature reduction, all the cells can be harvested as a single contiguous cell sheet with intact cell–cell junctions (Hirose *et al.*, 2000). Since the extracellular matrix deposited during culture is still retained underneath the harvested cell sheets (Kushida *et al.*, 1999), re-attachment of harvested cell sheets is reproducibly observed on various surfaces, including tissue surfaces and wound beds. These harvested cell sheets have been successfully applied in the clinical setting to treat corneal epithelium (Nishida *et al.*, 2004a, 2004b) and skin epidermis (Yamato *et al.*, 2001). When cell sheets are transplanted onto outer surfaces of the body, such as cornea and skin, the transplantation is easy and non-invasive. However, if large cell sheets need to be transplanted to internal organs, the procedure would be invasive.

Recently we have reported that tissue-engineered autologous fibroblast sheets were utilized for the closure of visceral pleural defects in rat (Kanzaki *et al.*, 2007) and porcine models (Kanzaki *et al.*, 2008). These defects caused intraoperative air leaks during pulmonary surgery; these often occur during cardiothoracic surgery, resulting in a decreased quality of life, since current methods,

*Correspondence to: Teruo Okano, Institute of Advanced Biomedical Engineering and Science, Tokyo Women's Medical University, 8-1 Kawada-cho, Shinjuku-ku, Tokyo 162-8666, Japan. E-mail: tokano@abmes.twmu.ac.jp

including the use of various biological and synthetic sealants, are often ineffective. In contrast to previous materials, such as fibrin glue, bioengineered cell sheets immediately and permanently seal air leaks in a dynamic fashion that allows the extensive tissue contraction and expansion involved in respiration without any postoperative recurrences. Additionally, mesothelial cells migrate to cover the transplanted cells sheets, thereby confirming excellent biocompatibility and integration with the host tissues (Kanzaki *et al.*, 2007). The tissue-engineered fibroblast sheets, having the flexibility to respond to expansion and contraction during respiration, were transplanted directly to the defects without the use of sutures or additional adhesive agents, such as fibrin glue (Kanzaki *et al.*, 2007, 2008).

In a previous study using a porcine animal model, thoracotomy, including temporal removal of a part of a rib, was performed, and cell sheets were transplanted using conventional forceps. However, in human clinical settings, less invasive thoracoscopic procedures, video-assisted thoracoscopic surgery (VATS), are often performed to eliminate large incisions and reduced hospitalization (Park *et al.*, 2008). Therefore, in the present study we developed a novel device to transplant cell sheets thoracoscopically through a tiny incision. We employed rapid prototyping techniques, including a three-dimensional (3D) computer-aided design (CAD) system and a 3D printer.

2. Materials and methods

All animal experiments were performed according to the *Guidelines of Tokyo Women's Medical University on Animal Use*, the *Principles of Laboratory Animal Care*, formulated by the National Society for Medical Research, and the *Guide for the Care and Use of Laboratory Animals*, prepared by the Institute of Laboratory Animal Resources and published by the National Institutes of Health (NIH Publication No. 86-23, revised 1985).

2.1. Temperature-responsive cell culture surfaces

Specific procedures for the preparation of square-patterned temperature-responsive cell culture dishes (provided by CellSeed, Tokyo, Japan) are described elsewhere (Hirose *et al.*, 2000). Briefly, *N*-isopropylacrylamide monomer in 2-propanol solution was spread onto 60 mm diameter polystyrene tissue culture dishes. The dishes were then irradiated with a 0.25 MGy electron beam, resulting in both polymerization and bonding onto the dish surfaces. PIPAAm-grafted dishes were rinsed with cold distilled water to remove unbonded monomer and dried in nitrogen gas. The PIPAAm-bonded surfaces were masked with a glass coverslip (24 × 24 mm) and irradiated after acrylamide (Wako Pure Chemicals, Osaka, Japan) was spread across the surface. The resulting culture dishes had central square areas bonded with temperature-responsive PIPAAm, with a surrounding border of non-cell adhesive polyacrylamide. These prepared dishes were sterilized using ethylene oxide gas.

2.2. Preparation of fibroblast sheets

Mouse embryonic fibroblasts (NIH/3T3) were obtained from Dainippon Pharmacy (Osaka, Japan). Cells were seeded onto square-patterned temperature-responsive culture dishes at an initial cell density of 3×10^5 cells/cm^2 and cultured for 3 days at 37 °C in a humidified atmosphere of 5% CO_2. The culture medium was Dulbecco's modified Eagle's medium (DMEM) supplemented with 5% fetal bovine serum, penicillin and streptomycin. After 3 days of culture, half of the medium was replaced with fresh culture medium containing 100 μg/ml ascorbic acid phosphate, and the cells were cultured for a further 4 days. After a total of 7 days of culture, confluent NIH/3T3 cells were stained with 100 ng/ml neutral red in Dulbecco's phosphate-buffered saline (PBS) for better visibility, and washed three times with PBS. The cells were stained with Trypan blue to determine viability and found to be viable. The stained NIH/3T3 cells were placed in another incubator at 20 °C for 30 min, and harvested as cell sheets.

2.3. Cell sheet transplantation device

The cell sheet transplantation device was designed for thoracoscopic surgery with CAD software (Inventor®, Autodesk, San Rafael, CA, USA) and the data were transferred to a rapid prototyping system (EDEN350™, Objet Geometries, Rehovot, Israel). Each part was made of a photopolymer (FullCure® 720, Objet Geometries), which is approved for medical use in terms of cytotoxicity, irritation, sensitization, USP Class VI, genotoxicity and Ames test.

2.4. Cell sheet transplantation

Ex vivo transplantation of cell sheets was performed using a pneumothrax model for VATS training (VATS Trainer™, Nihon Light Service, Tokyo, Japan), in which was placed excised porcine lung obtained from a slaughterhouse (Figure 1). A small piece of lung tissue (5 × 3 mm) was excised from the surface of right middle lobe of the lung. Three ports (Thoracoport™, Tyco Healthcare Japan, Tokyo, Japan) were placed on the chest wall of the model, one port (5.5 mm in diameter) for a general forceps to assist cell sheet transplantation, and two ports (12 mm in diameter) for a thoracoscope and the cell sheet transplantation device. After temperature reduction, most culture medium was removed and a support paper membrane (SS25, Asahikasei, Tokyo, Japan) was placed on the cells. Since the support membrane absorbed the remaining culture medium, the membrane attached to the apical cell surfaces by surface tension. Then, the wetted

DOI: 10.1002/term

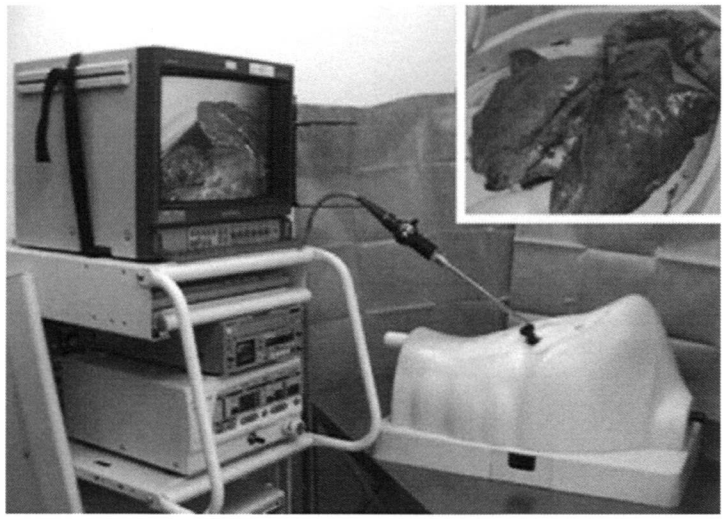

Figure 1. *Ex vivo* **cell sheet transplantation. A porcine lung (upper right inset) was placed in a human body pneumothrax model for VATS training. Three ports were used, for the cell sheet transplantation device, a conventional forceps and a thoracoscope**

support membrane with a cell sheet was placed on the film of the device. According to the surface tension of the adsorbed medium, the support membrane was stably fixed on the membrane.

3. Results

The cell sheet transplantation device was designed for thoracoscopic surgery and composed of a square elastic film (75 μm thick × 28 mm × 40 mm) connected to a shaft (10 mm in outer diameter), a dial and an outer sheath (12 mm in outer diameter) fixed with a grip (Figure 2a). The elastic film and the outer sheath were made of medical-grade polyethylene (fluoropolymer, 2.9 Mil, Medical Release Liner 9956, 3M, Maplewood, MN, USA) and polycarbonate, respectively. The other parts were fabricated with a photopolymer approved for medical use in a rapid prototyping system. Since the shaft and dial have a pair of gears between them (Figure 2b), a surgeon can pull the shaft out of the sheath and push it back inside just by revolving the dial with a finger. The grip can rotate 360° around the axis of the shaft. Since elasticity of the film was optimized, the film on which a cell sheet was placed was easily pulled and stored inside the shaft (Figures 2c–e). Therefore, the cell sheet in the device was delivered though a tiny port which protected it from physical damage.

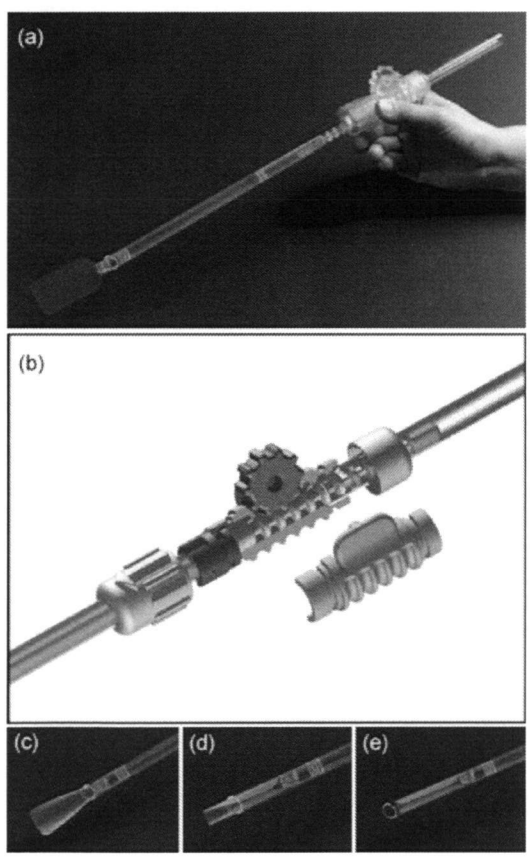

Figure 2. Cell sheet transplantation device. All the parts except for the elastic membrane and the sheath were made of a photopolymer approved for medical use and fabricated with a rapid prototyping system (a). Since the shaft and the dial have a pair of gears between them, the shaft is pulled out of the sheath and pushed back inside just by revolving the dial (b–e)

Fibroblast sheets were harvested with supporter paper membranes after cell staining, then placed on the elastic films (Figure 3). In the present study, the shaft containing a cell sheet was inserted from the 12 mm port in the training model's chest wall to the wound site of the lung. All the procedures in the model were monitored thoracoscopically (Figure 4). Upon pushing the elastic film outside the shafts, the film spread immediately (Figures 4a–c). Then, the cell sheet and the overlying support membrane on the elastic film were placed on the wound site and the film was rubbed with an assisting forceps (Figure 4d). By gently lifting up the

DOI: 10.1002/term

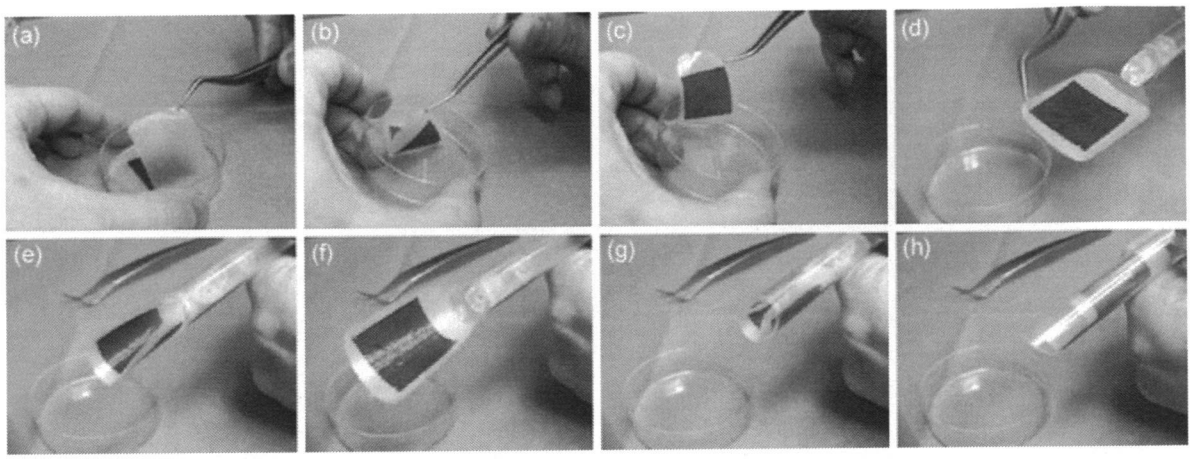

Figure 3. Storing a cell sheet in the device. Cell sheets were harvested with support paper membranes (a–c), and placed on the elastic films (d). Then, the films were stored inside the shafts (e–h)

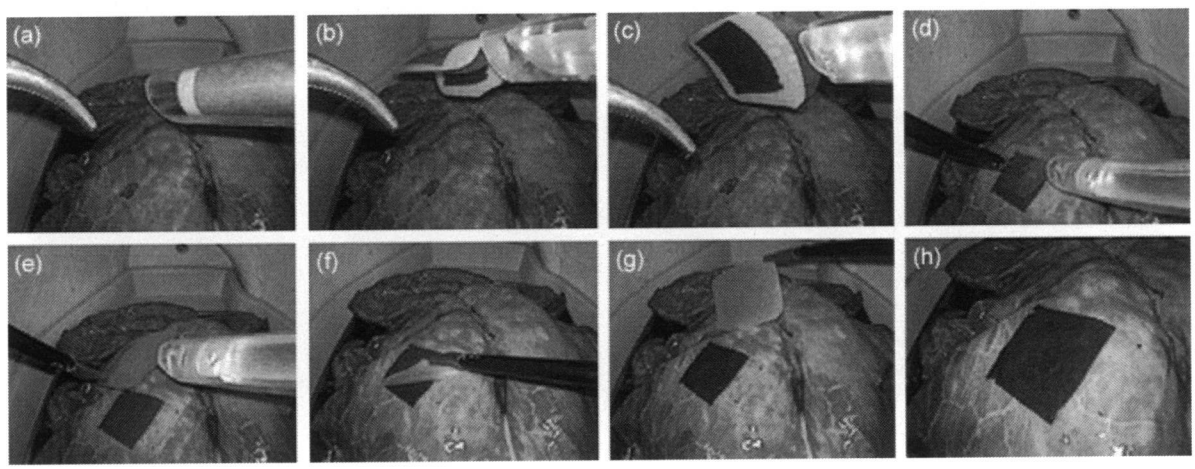

Figure 4. Thoracoscopic view of cell sheet transplantation with the device. Cell sheets were placed on the wound sites (a–c), then the cell sheets were successfully transferred to lung surfaces by rubbing the elastic films with a general forceps (d). After detaching the elastic films (e), the support membranes were peeled off the transplanted cell sheets (f–h)

shaft connected with elastic film, the elastic film was detached from the support paper membrane (Figure 4e). Then the support membrane was peeled from the cell sheet with general grasping forceps (Figures 4f–h). These procedures were reproducibly and successfully performed after 7 min of contact of the cell sheets with the lung surfaces. In the previous study using open surgery, 5 min of contact was sufficient for fibroblast sheets to create strong adhesion, resistant to peeling with forceps (Kanzaki *et al.* 2007, 2008). This is probably due to abundant extracellular matrix deposited in the fibroblast sheets. Finally, the shaft was stored inside the sheath and withdrawn from the body. The entire procedure for single cell sheet transplantation took around 10 min.

4. Discussion

Here, a novel cell sheet transplantation device for thoracoscopic surgery was developed in a rapid prototyping manner, using a CAD system and a 3D printer. Since it took <1 h to produce all the parts of the device, quick turnaround was easily achieved. When faults or shortcomings were observed, the design was quickly changed using a 3D CAD system, and new parts were produced. For example, the shaft did not rotate, since a rack and pinion was used in the original design; however, when thoracoscopists needed rotation during experiments, the rack and pinion was replaced with another type of gear (Figure 2b). The design, including a pair of gears and a grip, was changed six times within a few weeks. Such rapid optimization was never achieved without a rapid prototyping system.

Since cell sheets fabricated on temperature-responsive surfaces are scaffold-free and the thickness is usually <200 μm, the sheets could often be rumpled and damaged when grasped directly with forceps. Once cell sheets are rumpled, it is not easy to expand them again without tearing or breakage outside the culture medium. Therefore, support membranes are often utilized for cell

sheet transplantation (Hirose *et al.*, 2000; Kanzaki *et al.*, 2007, 2008; Ohashi *et al.*, 2007; Ohki *et al.*, 2006). Three types of elastic films commercially available for medical use were tested, and we found that only one film achieved both holding the support membranes with cell sheets by water surface tension during delivery and its storage inside the sheath.

5. Conclusions

The newly designed device for cell sheet transplantation was fabricated in a rapid prototyping manner. The results of *ex vivo* thoracoscopic cell sheet transplantation revealed that this device would be suitable for performing cell sheet transplantation in minimally invasive thoracoscopic surgery.

Acknowledgements

We gratefully acknowledge Professor Takamasa Onuki (Department of Surgery I, Tokyo Women's Medical University) for surgical expertise and are grateful to Dr Kyojiro Nambu (Department of Radiology, Tokyo Women's Medical University; Toshiba Medical Systems) for his advice. We are also grateful to Yoshihiro Muragaki, Ryoichi Nakamura, Takashi Suzuki, Shigeru Nagai, Ryo Takagi and Daisuke Murakami for helpful technical assistance and advice. This work was supported by the High-Tech Research Centre Programme and the Formation of Innovation Centre for Fusion of Advanced Technologies in the Special Coordination Funds for Promoting Science and Technology, from the Ministry of Education, Culture, Sports, Science and Technology (MEXT), Japan.

References

Hirose M, Kwon OH, Yamato M, *et al.* 2000; Creation of designed shape cell sheets that are noninvasively harvested and moved onto another surface. *Biomacromolecules* **1**: 377–381.

Kanzaki M, Yamato M, Yang J, *et al.* 2007; Dynamic sealing of lung air leaks by the transplantation of tissue engineered cell sheets. *Biomaterials* **28**: 4294–4302.

Kanzaki M, Yamato M, Yang J, *et al.* 2008; Functional closure of visceral pleural defects by autologous tissue engineered cell sheets. *Eur J Cardiothorac Surg* **34**: 864–869.

Kushida A, Yamato M, Konno C, *et al.* 1999; Decrease in culture temperature releases monolayer endothelial cell sheets together with deposited fibronectin matrix from temperature-responsive culture surfaces. *J Biomed Mater Res* **45**: 355–362.

Nishida K, Yamato M, Hayashida Y, *et al.* 2004a; Functional bioengineered corneal epithelial sheet grafts from corneal stem cells expanded *ex vivo* on a temperature-responsive cell culture surface. *Transplantation* **77**: 379–385.

Nishida K, Yamato M, Hayashida Y, *et al.* 2004b; Corneal reconstruction with tissue-engineered cell sheets composed of autologous oral mucosal epithelium. *N Engl J Med* **351**: 1187–1196.

Ohashi K, Yokoyama T, Yamato M, *et al.* 2007; Engineering functional two- and three-dimensional liver systems *in vivo* using hepatic tissue sheets. *Nat Med* **13**: 880–885.

Ohki T, Yamato M, Murakami D, *et al.* 2006; Treatment of oesophageal ulcerations using endoscopic transplantation of tissue-engineered autologous oral mucosal epithelial cell sheets in a canine model. *Gut* **55**: 1704–1710.

Park BJ, Flores RM. 2008; Cost comparison of robotic, video-assisted thoracic surgery and thoracotomy approaches to pulmonary lobectomy. *Thorac Surg Clin* **18**: 297–300, vii.

Yamada N, Okano T, Sakai H, *et al.* 1990; Thermo-responsive polymeric surfaces; control of attachment and detachment of cultured cells. *Makromol Chem Rapid Commun* **11**: 571–576.

Yamato M, Utsumi M, Kushida A, *et al.* 2001; Thermo-responsive culture dishes allow the intact harvest of multilayered keratinocyte sheets without dispase by reducing temperature. *Tissue Eng* **7**: 473–480.

Yang J, Yamato M, Okano T. 2005; Cell-sheet engineering using intelligent surfaces. *MRS Bull* **30**: 189–193.

Analysis of soluble vascular endothelial growth factor receptor-1 secreted from cultured corneal and oral mucosal epithelial cell sheets in vitro

S Kanayama,[1] K Nishida,[2] M Yamato,[3] R Hayashi,[2] N Maeda,[4] T Okano,[3] Y Tano[4]

[1] Department of Ophthalmology, University of Washington Medical Center, Seattle, Washington, USA; [2] Department of Ophthalmology and Visual Science, Tohoku University Graduate School of Medicine, Sendai, Japan; [3] Institute of Advanced Biomedical Engineering and Science, Tokyo Women's Medical University, Tokyo, Japan; [4] Department of Ophthalmology, Osaka University Medical School, Suita, Japan

Correspondence to:
Dr S Kanayama, Department of Ophthalmology, University of Washington Medical Center, 1959 NE Pacific Street, HSC RR810, Seattle, WA 98195, USA; kanayama@ophthal.med.osaka-u.ac.jp

Accepted 24 June 2008

ABSTRACT

Background: In clinical trials, eyes transplanted with cultured oral mucosal epithelial cell sheets have shown increased neovascularisation compared with eyes treated with cultured corneal epithelial cell sheets. As reported recently, soluble vascular endothelial growth factor receptor-1 (soluble VEGFr-1) is a main factor to maintain a corneal avascularity.

Aim: To investigate soluble VEGFr-1 of cultured corneal epithelial cells (CCE) and cultured oral mucosal epithelial cells (COE) in vitro.

Methods: Rabbit corneal and oral mucosal epithelial cells were co-cultured with mitomycin C-treated NIH/3T3 cells on culture plates. After CCE and COE were multilayered, culture medium was replaced by basal medium and incubated. Protein secretion of soluble VEGFr-1 was assessed in conditioned medium from CCE and COE by ELISA. Angiogenic potential was examined by invasion, migration assays with human umbilical vein endothelial cells (HUVECs) in addition to recombinant soluble VEGFr-1.

Results: CCE secreted a significantly higher amount of soluble VEGFr-1 than did COE. Recombinant soluble VEGFr-1 significantly suppressed HUVEC migration induced by COE, without suppression in CCE. In conclusion, these findings suggest that low protein levels of soluble VEGFr-1 may lead to corneal neovascularisation after COE sheet transplantation.

Limbal epithelial stem cells are completely lost in patients who are affected by ocular trauma, thermal and chemical burns, and severe eye disease such as Stevens–Johnson syndrome and ocular pemphigoid. Consequently, contiguous conjunctival epithelia cover the cornea, leading to corneal vascularisation and opacification with severe visual loss. Recently, patients with unilateral limbal stem cell deficiency have also received corneal epithelial grafts ex vivo by the expansion of autologous limbal stem cells harvested from healthy contralateral eyes, [1] as well as limbal epithelial cells cultured on cell carrierrs such as amniotic membrane[2–4] and temperature-responsive culture surfaces.[5] In patients with bilateral limbal stem cell deficiency, tissue-engineered epithelial cell sheets composed of the patient's own oral mucosal epithelial cells have also been developed recently to avoid the need for allogenic donor tissues.[6 7] Using autologous oral mucosal epithelial cells, those patients with bilateral stem cell deficiencies are not required to take immune-suppressing drugs for a long time to prevent the postoperative rejection of transplantation with severe side effects such as renal dysfunction and malignant lymphoma.

However, eyes transplanted with cultured oral mucosal epithelial cell (COE) sheets have shown increased neovascularisation compared with eyes transplanted with cultured corneal epithelial cell (CCE) sheets. This vascularisation occurred just beneath the cultured oral mucosal epithelial cell sheets, via invasion from the peripheral cornea.[6]

Corneal avascularity appears to be reliant on a balance between several angiogenic factors and antiangiogenic factors, such as antiangiogenic molecules including thrombospondin-1 (TSP-1) and endostatin.[8] In particular, soluble vascular endothelial growth factor receptor-1 (soluble VEGFr-1) was essential to corneal avascularity in a variety of animal models.[9] Soluble VEGFr-1 has been shown to be antiangiogenic by acting as a decoy receptor for secreted VEGF and also inactivating membrane-bound VEGF receptors 1 and 2 by heterodimerisation. We have shown that the secretion of VEGF protein levels was approximately equal between CCE and COE.[10] We postulate that the protein expression of soluble VEGFr-1 by CCE was greater than by COE, as a decoy for VEGF. In relative terms, the angiogenic-induction capabilities of COE were higher than that of CCE. We investigated the quantification of protein levels of soluble VEGFr-1 in the conditioned medium.

There are several crucial steps in the angiogenic process. The initial step is stimulation of endothelial cells by angiogenic factors. The second step is to invade cell membrane structure and then to increase vascular permeability (cell invasion). The third step is to create an environment supporting endothelial migration due to extravasation of plasma proteins (cell migration). The last step is to form cords and subsequently a lumen, and to recruit pericytes to stabilise the new vessel structure. In the second study, soluble VEGFr-1 was added to block endothelial cell invasion and migration.

MATERIALS AND METHODS

Animals

New Zealand White Rabbits (male, 1.5–2.0 kg) were purchased from Kitayama Labs (Nagano, Japan). Rabbits were treated in accordance with the ARVO statement for the use of Animals in Ophthalmic and Vision Research. All biopsies were taken from rabbits under deep anaesthesia with an intramusclar injection of xylazine hydrochloride (4 mg/kg) and ketamine hydrochloride (40 mg/kg).

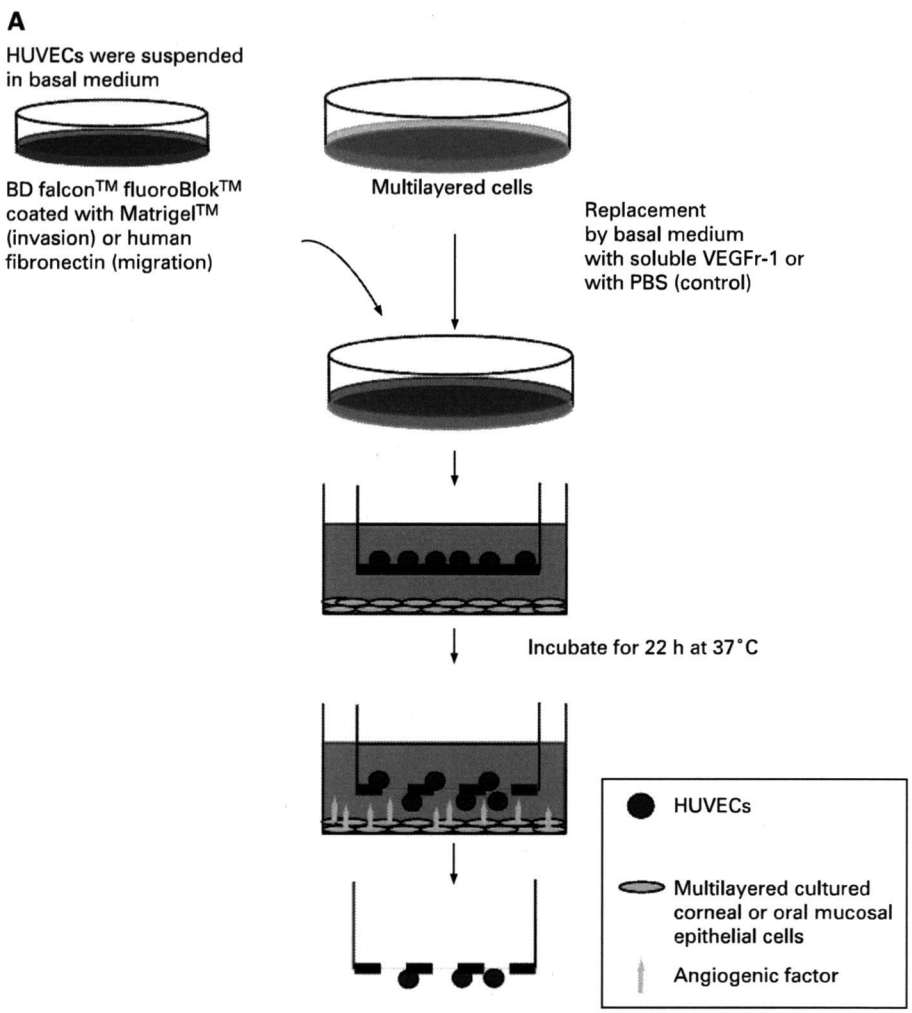

Figure 1 Cell invasion and migration assay with addition of soluble vascular endothelial growth factor receptor-1 (soluble VEGFr-1). Corneal and oral mucosal biopsies were taken from rabbits, and epithelial layers were removed with forceps and treated to create single cell suspensions. Suspended cells were cocultured with mitomycin C-treated NIH/3T3 cells on 24-well culture plates. After cultured corneal epithelial cells (CCE) and cultured oral mucosal epithelial cells (COE) were multilayered on the lower chambers, the culture medium was replaced by the basal medium containing 1 μg/ml recombinant soluble VEGFr-1 or phosphate-buffered saline (PBS) as a control. A total of 5% fetal bovine serum (FBS) in the lower chamber without cultured epithelial cells was used as a positive control. Suspended human umbilical vein endothelial cells (HUVECs) were added to each of the top chambers at densities of 5×10^4 and 2×10^4 cells for invasion (N = 4) and migration (N = 4) assays, respectively. Both chambers were incubated for 22 h at 37°C to induce invasion or migration. Values were expressed as relative percentages in comparison with the 5% FBS positive control. (A) Micrographs of CCE (B) and COE (C) were taken under a phase-contrast light microscope at 200× magnification. Scale bar, 100 μm.

Cell culture

Human umbilical vein endothelial cells (HUVECs) were purchased from Kurabo Industries (Osaka, Japan) and grown in basal medium (Humedia-EB2; Kurabo) containing supplements and serum (Humedia-EG; Kurabo). All experiments used endothelial cells between passages 2 and 5. Corneal and oral mucosal biopsies were taken from rabbits and washed twice with 0.5% povidone–iodine solution and once with phosphate-buffered saline (PBS) (Nikken Biomedical Laboratory, Kyoto, Japan) containing antibiotics and antimycotics. Corneal biopsies were incubated for 1 h at 37°C in Dulbecco modified Eagle medium (DMEM) containing 2.4 U/ml dispase (Gibco, Grand Island, New York), and oral mucosal biopsies were incubated for 4 h at 4°C in DMEM containing 1000 U/ml dispase (Godo Shusei, Tokyo). Corneal and oral mucosal epithelial layers were removed with forceps and treated with trypsin-EDTA solution (Gibco) for 20 min at 37°C to create single cell suspensions. Suspended cells were co-cultured with mitomycin C (MMC)-treated NIH/3T3 cells on 24-well culture plates (353047, BD Biosciences, Franklin Lakes, New Jersey). After culturing for 2 weeks, CCE and COE were mutilayered.

Enzyme-linked immunosorbent assay

Protein levels of soluble VEGFr-1 in the conditioned medium of CCE and COE (N = 6) were quantified.[11] Conditioned medium from multilayered CCE or COE was obtained after culture in

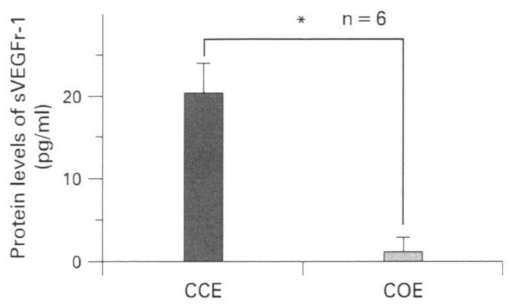

Figure 2 Qunatification of soluble vascular endothelial growth factor receptor-1 (sVEGFr-1) secretion. To quantify protein levels of sVEGFr-1 produced by the cultured corneal epithelial cells (CCE) and cultured oral mucosal epithelial cells (COE), conditioned medium from both cell sources were examined by ELISA. Secreted levels of soluble VEGFr-1 by CCE were significantly higher than by COE (20.4 (3.6) pg/ml and 1.2 (1.6) pg/ml, N = 6; $p<0.05$).

the basal medium for 22 h at 37°C and then quantified using enzyme-linked immunosorbent assay (ELISA) kits (Quantikine, R&D Systems, Mineapolis, Minnesota) according to the manufacturer's suggested protocol.

Cell invasion and migration assay with addition of soluble VEGFr-1

Cell invasion assays were performed using the BD BioCoat Angiogenesis System for Endothelial Cell Invasion (354141, BD Biosciences), and migration assays were conducted with the BD BioCoat Angiogenesis System for Endothelial Cell Migration (354143, BD Biosciences). Recombinant soluble VEGFr-1 (Fitzgerald Industries International, Concord, Massachusetts) was used to block endothelial cell invasion and migration. After CCE and COE were multilayered on the lower chambers, the culture medium was replaced by the basal medium containing 1 μg/ml of recombinant soluble VEGFr-1 or PBS as a control. Five per cent fetal bovine serum (FBS) in the lower chamber

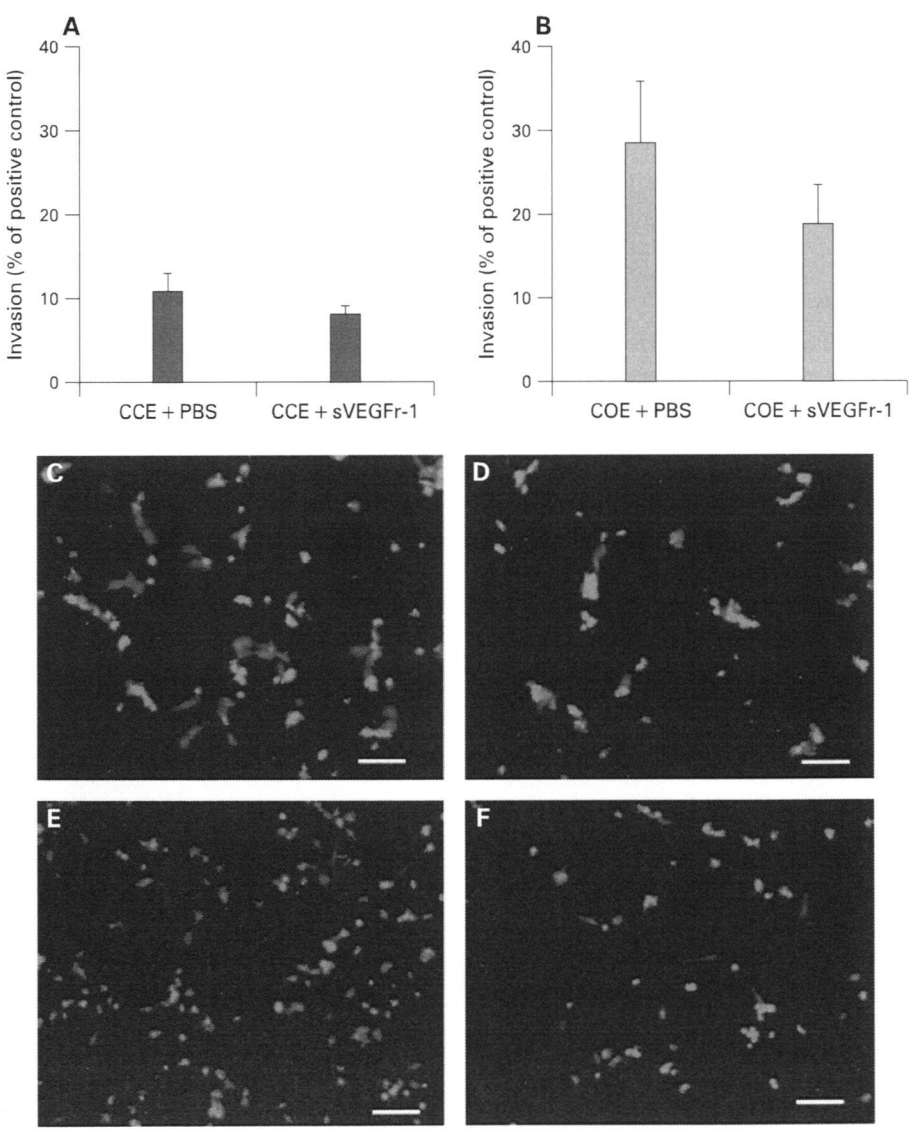

Figure 3 Blocking cell invasion using recombinant soluble vascular endothelial growth factor receptor-1 (sVEGFr-1). To determine the effects of the sVEGFr-1 against the angiogenic potential of the cultured epithelia, sVEGFr-1 was examined for its potential to reduce human umbilical vein endothelial cell (HUVEC) invasion towards cultured corneal epithelial cells (CCE) and cultured oral mucosal epithelial cells (COE). Invasion of HUVECs toward CCE with sVEGFr-1 was not suppressed significantly compared with the control (10.7 (2.2)% and 8.0 (1.1)%, N = 4, $p>0.05$) (A). Invasion of HUVECs toward COE was suppressed to 66% compared with the control, but this difference was beyond the significant level (28.6 (7.3)% and 18.8 (4.7)%, N = 4, $p>0.05$) (B). Fluorescence microscopy (100×) demonstrated invasion of HUVECs through Matrigel-coated membranes toward CCE with phosphate-buffered saline (PBS) (control) (C) and with soluble VEGFr-1(D), toward COE with PBS (E) and with soluble VEGFr-1(F). Scale bar, 100 μm.

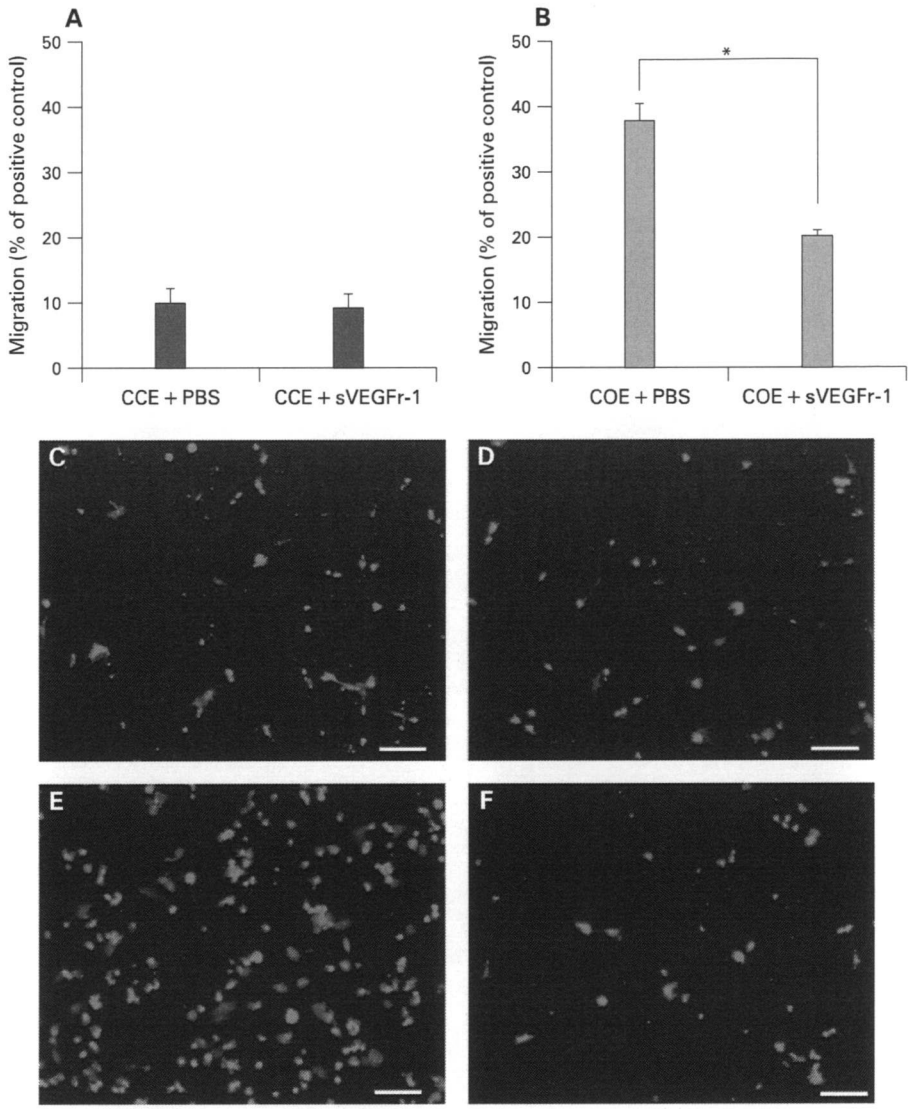

Figure 4 Blocking cell migration using recombinant soluble vascular endothelial growth factor receptor-1 (sVEGFr-1). For human umbilical vein endothelial cell (HUVEC) migration, no significant suppression by the soluble VEGFr-1 was detected toward cultured corneal epithelial cells (CCE) (10.1 (2.2)% and 9.1 (2.1)%, N = 4, $p>0.05$) (A). However, sVEGFr-1 showed significant suppression of HUVEC migration toward cultured oral mucosal epithelial cells (COE) (37.6 (2.9)% and 20.0 (0.8)%, N = 4, $p<0.05$) (B). Migration of HUVECs through fibronectin-coated membranes was observed toward CCE with phosphate-buffered saline (PBS) (C) and soluble VEGFr-1 (D) and towards COE with PBS (E) and with soluble VEGFr-1 (F), with a greater number of HUVECs apparently to block migrating towards COE with soluble VEGFr-1 in fluorescence microscopy (100×). Scale bar, 100 μm.

without cultured epithelial cells was used as a positive control. HUVECs starved of serum for 4 h were treated with trypsin-EDTA and resuspended in the basal medium. Suspended HUVECs were added to each of the top chambers at densities of 5×10^4 and 2×10^4 cells for invasion (N = 4) and migration (N = 4) assays, respectively. Both chambers were incubated for 22 h at 37°C to induce invasion through the Matrigel-coated membranes or migration through fibronectin-coated membranes. The top chambers were then transferred to wells containing Calcein AM (Dojindo Lab, Kumamoto, Japan) in Hanks balanced salt solution for 1.5 h at 37°C and measured with a fluorescence plate reader (ARVO1420, Perkin Elmer, Massachusetts) at 485/530 nm (fig 1A). Both the CCE (fig 1B) and the COE (fig 1C) had a normal epithelial morphology in phase-contrast micrographs after both were multilayered on 24-well plates.

Values were expressed as relative percentages in comparison with the 5% FBS positive control.

Statistical analysis

Data are presented as the mean (SE). Statistical significance was analysed using the Mann–Whitney test. A p value of less than 0.05 was considered significant.

RESULTS

Quantification of soluble VEGFr-1 in conditioned medium from CCE and COE

To quantify the protein levels of soluble VEGFr-1 produced by the CCE and COE, conditioned medium from both cell sources was examined by ELISA. Secreted levels of soluble VEGFr-1 by CCE were significantly higher than by COE (20.4 (3.6) pg/ml and 1.2 (1.6) pg/ml, N = 6; $p<0.05$) (fig 2).

Effect of soluble VEGFr-1 in cell invasion and migration assay

To determine the effects of the soluble VEGFr-1 against the angiogenic potential of the cultured epithelia, soluble VEGFr-1 was examined for its potential to reduce HUVEC invasion and migration towards CCE and COE. Invasion of HUVECs toward CCE with recombinant soluble VEGFr-1 was not suppressed significantly compared with the control (10.7 (2.2)% and 8.0 (1.1)%, N = 4, $p>0.05$) (fig 3A). Invasion of HUVECs toward COE was suppressed to 66% compared with the control, but this difference was out of the significant level (28.6 (7.3)% and 18.8 (4.7)%, N = 4, $p>0.05$) (fig 3B). For HUVEC migration, no significant suppression by the soluble VEGFr-1 was detected toward CCE (10.1 (2.2)% and 9.1 (2.1)%, N = 4, $p>0.05$)

(fig 4A). However, soluble VEGFr-1 showed a significant suppression of HUVEC migration toward COE (37.6 (2.9)% and 20.0 (0.8)%, N = 4, $p<0.05$) (fig 4B). Representative photographs of fluorescence microscopy demonstrate the invasion of HUVECs toward CCE with PBS (fig 3C), with soluble VEGFr-1 (fig 3D), toward COE with PBS (fig 3E) and with soluble VEGFr-1 (fig 3F). Similarly representative migration of HUVECs through fibronectin-coated membranes was also observed toward CCE with PBS (fig 4C) and with soluble VEGFr-1 (fig 4D) and towards COE with PBS (fig 4E) and with soluble VEGFr-1 (fig 4F). A greater number of migrating HUVECs were apparently blocked towards COE with soluble VEGFr-1.

DISCUSSION

In the present study, we confirmed that secreted levels of soluble VEGFr-1 by CCE were significantly higher than by COE. This result indicates that the antiangiogenic activity of soluble VEGFr-1 plays a role in the occurrence of corneal avascularity after transplantation of CCE sheet. Based on the expression of soluble VEGFr-1, we showed that the characteristics of corneal epithelial cells were unchanged even if cultured ex vivo.

Further, invasion of HUVECs toward CCE was blocked by 25% with soluble VEGFr-1, in comparison with the control. Similarly, migration of HUVECs toward CCE was blocked by only 10% with soluble VEGFr-1. The suppression rates of HUVEC invasion and migration using soluble VEGFr-1 toward COE were 66% and 53%. We have previously demonstrated that the protein secretion of VEGF was similar for CCE and COE.[10] In combination with these results, corneal neovascularisation after COE transplantation might occur due to a small degree of secretion of soluble VEGFr-1, which acts as an endogenous VEGF trap, from COE.

Recently, we have described that FGF2, among the various angiogenic factors, played one of the factors in corneal angiogenesis after transplantation of COE sheets.[10] Sekiyama *et al* have recently described that TSP-1, an antiangiogenic factor, plays an important role in the inhibition of angiogenesis after CCE sheets.[12] Also, soluble VEGFr-1 contributes to the corneal antiangiogenic barrier.[13] As a result of the low degree of expression of soluble VEGFr-1 from COE, VEGF protein expression from COE could not be inhibited by soluble VEGFr-1. Consequently, soluble VEGFr-1 plays an important role in corneal angiogenesis after transplantation of COE sheets indirectly. However, there is a possibility of relating other angiogenic or antiangiogenic factors with corneal neovascularisation after transplantation of the COE sheet. In addition, we postulate that corneal neovascularisation after transplantation of the COE sheet may be affected by the imbalance between multiple angiogenic factors and antiangiogenic factors, rather than a single factor.

Therefore, in subsequent studies, we aim to develop new devices to reduce corneal neovascularisation after COE sheet transplantation using combination therapies of both FGF2 neutralising antibodies and recombinant soluble VEGFr-1.

Acknowledgements: The authors thank N O Masuda for useful and technical comments.

Funding: This work was supported by The Osaka Medical Research Foundation for Incurable Diseases in Japan.

Competing interests: None.

REFERENCES

1. **Pellegrini G,** Traverso CE, Franzi AT, *et al.* Long-term restoration of damaged corneal surfaces with autologous cultivated corneal epithelium. *Lancet* 1997;**349**:990–3.
2. **Schwab IR,** Reyes M, Isseroff RR. Successful transplantation of bioengineered tissue replacements in patients with ocular surface disease. *Cornea* 2000;**19**:421–6.
3. **Shimazaki J,** Aiba M, Goto E, *et al.* Transplantation of human limbal epithelium cultivated on amniotic membrane for the treatment of severe ocular surface disorders. *Ophthalmology* 2002;**109**:1285–90.
4. **Tsai RJ,** Li LM, Chen JK. Reconstruction of damaged corneas by transplantation of autologous limbal epithelial cells. *N Engl J Med* 2000;**343**:86–93.
5. **Nishida K,** Yamato M, Hayashida Y, *et al.* Functional bioengineered corneal epithelial sheet grafts from corneal stem cells expanded ex vivo on a temperature-responsive cell culture surface. *Transplantation* 2004;**77**:379–85.
6. **Inatomi T,** Nakamura T, Koizumi N, *et al.* Current concepts and challenges in ocular surface reconstruction using cultivated mucosal epithelial transplantation. *Cornea* 2005;**24**:32–8S.
7. **Nishida K,** Yamato M, Hayashida Y, *et al.* Corneal reconstruction with tissue-engineered cell sheets composed of autologous oral mucosal epithelium. *N Engl J Med* 2004;**351**:1187–96.
8. **Chang JH,** Gabison EE, Kato T, *et al.* Corneal neovascularization. *Curr Opin Ophthalmol* 2001;**12**:242–9.
9. **Ambati BK,** Nozaki M, Singh N, *et al.* Corneal avascularity is due to soluble VEGF receptor-1. *Nature* 2006;**443**:993–7.
10. **Kanayama S,** Nishida K, Yamato M, *et al.* Analysis of angiogenesis induced by cultured corneal and oral mucosal epithelial cell sheets in vitro. *Exp Eye Res* 2007;**85**:772–81.
11. **Ohtani K,** Egashira K, Hiasa K, *et al.* Blockade of vascular endothelial growth factor suppresses experimental restenosis after intraluminal injury by inhibiting recruitment of monocyte lineage cells. *Circulation* 2004;**110**:2444–52.
12. **Sekiyama E,** Nakamura T, Kawasaki S, *et al.* Different expression of angiogenesis-related factors between human cultivated corneal and oral epithelial sheets. *Exp Eye Res* 2006;**83**:741–6.
13. **Ambati BK,** Patterson E, Jani P, *et al.* Soluble vascular endothelial growth factor receptor-1 contributes to the corneal anti-angiogenic barrier. *Br J Ophthalmol* 2007;**91**:505–8.